Supporting Information

Eutrophication increases phytoplankton methylmercury concentrations in a coastal sea - a Baltic Sea case study

Anne. L. Soerensen[a*], Amina T. Schartup[b], Erik Gustafsson[c], Bo G. Gustafsson[c], Emma Undeman[a,c], Erik Björn[d]

[a] *Stockholm University, Department of Environmental Science and Analytical Chemistry, Stockholm, Sweden*
[b] *Harvard University, John A. Paulson School of Engineering and Applied Sciences, Cambridge MA, USA*
[c] *Stockholm University, Baltic Nest Institute, Baltic Sea Centre, Stockholm, Sweden*
[d] *Umeå University, Department of Chemistry, Umeå, Sweden*

* corresponding author (e-mail: anne.soerensen@aces.su.se; phone: +46 86747278)

Content

1) Text S1: Extended methods 2014 field campaign
2) Figure S1: Structure of depth layers in Baltsem
3) Text S2: Detailed description of the historic river Hg inventory
4) Table S1: Basin specific river Hg discharge, Hg:TOC ratios and TSS
5) Figure S2: MeHg – salinity correlation
6) Figure S3: BAF – mPOM correlation
7) Figure S4: Historic loads of N, P, and Hg to the Baltic Sea
8) Figure S5: 2014 cruise track and observations
9) Figure S6: Model evaluation (total Hg and total MeHg)
10) Figure S7: Model evaluation (Hg^0)
11) Figure S8: Model evaluation (total Hg sediment)
12) Table S2: Above halocline Hg concentrations
13) Table S3: Model parameterizations: Particles
14) Table S4: Model parameterizations: Water chemistry
15) Table S5: Model parameterizations: Sediment
16) Table S6: Model parameterizations: Evasion

Text S1: 2014 MeHg observations

Field sampling. Figure S1 shows the September 2014 seawater sampling stations for Hg species in the Baltic Sea. Methylated Hg (MeHg+Me_2Hg) was determined in unfiltered water samples collected at 2-8 depths at each station. MeHg samples were collected from the ships rosette bottles. All samples (125 ml) were spiked with 0.03 pmol $Me^{200}Hg$ isotope standard for later isotope dilution analysis and then acidified to 0.1 M HCl using trace metal grade 30% HCl. Samples were analyzed using thermal desorption gas chromatography inductively coupled plasma mass spectrometry (TDGC-ICPMS) after direct ethylation with sodium tetraethylborate and purge and trap on tenax adsorbent following the isotope dilution analysis procedure of Lambertsson and Björn[1] and the sample treatment procedure of Munson and Lamborg.[2] We removed contribution to samples from handling by subtracting the difference (10 fM) between field blank (20±5 fM, n=12) and MQ water sample levels (10±7 fM, n=43) from all observations. The detection limit (LOD) was determined to 13 fM based on three times standard deviation of replicated (n=12) field blanks. In order to calculate averages observations below the detection limit was set to 50% of the level of detection. For triplicate samples in waters with methylated Hg concentrations above the detection limit the standard deviation of samples were 10% of the average.

Incubation experiments. At six stations (3-4 depths) incubations experiments where performed on board in order to determine the rate constants for dark Hg^{II} methylation and MeHg demethylation in water samples. We measured methylation and demethylation rates using incubation in the dark for 24 hours at room temperature (20°C) for samples with water temperature >8 °C and at 4°C for samples with water temperature <8°C in order to best replicate the environment that the samples were collected in. Each sample bottle (250 ml) was spiked with 0.06 pmol $Me^{199}Hg$ and 62 pmol $^{198}Hg(II)$ at the start of the experiment. Each station and depth had two bottles, one that was acidified with trace metal grade 30% HCl (1%) at time zero (t0) and one that was acidified after 24 hours. Immediately after acidification (i.e. the termination of the incubation) samples were spiked with 0.06 pmol $Me^{200}Hg$ standard for isotope dilution analysis. Samples were analyzed using TDGC-ICPMS as described above. Concentrations of methylated Hg for ambient Hg and tracers were then calculated from mass-bias corrected signals using signal deconvolution.[3]

Detection limit for the rate constant for dark demethylation (3% d^{-1}) was calculated according to Hintelmann and Evans.[4] For the methylation rate constant the detection limit was calculated as 3×the standard deviation of the determined $Me^{198}Hg$ concentration in all t0 samples. This approach was necessary to account for the increased uncertainty caused by a

fraction of $^{198}Hg^{II}$ being methylated in the direct ethylation derivatization reaction. To get a conservative estimate of the average demethylation rate constant we set the measured rate constants below the detection limit to zero (48% of samples). This result in an average rate constant of 5.5±6.2 % d^{-1}.

Ancillary data. Temperature, salinity, oxygen concentration, sulfide concentration, phosphorous concentration, nitrate concentration, ammonium concentration, total nitrogen concentration, and silicate concentration were collected by the Swedish Meteorological Institute (SMHI) and quality controlled based on their standard procedure.

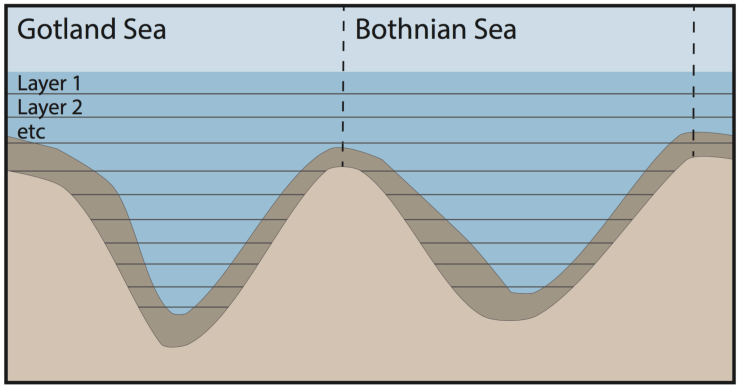

Figure S1. Illustration of the structure of water and sediment layers/compartments in each basin in the Baltsem model.

Text S2: River Hg discharge

We created a historic (1850-present) Hg river discharge inventory. From 1850 to 1975 we assume a linear increase from 50% of present day discharge in 1850 to 10 times that of present day discharge in 1940 and then steady Hg river inputs until 1975. This distribution matches the general distribution from Horowitz[5] and are validated by comparison to dated sediment cores from several Baltic Sea sub-basins that show natural background concentrations (20-40 μg kg^{-1}) until the early 1900s despite a start of the industrialization in northern Europe around 1850 [6]. For 1975 to 2010 we combine information from different types of reported measurements. We use the decline in Swedish sewage sludge between 1987 and 1995 and extrapolate back to 1975 (-7.5% y^{-1} between 1987 and 1995)[7]. This trends correspond to the general decline for Europe suggested by Amos et al.[8] We use the relative change in total Hg (-40% period /-3.2% y^{-1}) seen in both discharge from Swedish rivers between 1995-1997 (4.3±3.9 ng l^{-1}) to 2011-2013 (2.2±1.1 ng l^{-1}) and in sludge from Swedish waste water treatment plants[9, 10] to create a 1995 to 2012 trend.

While we assume that most point sources are reflected in our historic river inventory we include one large coastal smelting plant (Rönnskärsverken) known to be responsible for polluting a large area of sediments in the Bothnian Bay in especially the 1960s separately (see figure below). We predict that Rönnskärsverken contribute around 20-25% of all external Hg inputs to the Baltic Sea in the 1960s.

A study on submarine groundwater discharge of Hg in the Southern Baltic Sea found that this source was substantially lower than river discharge[11] and it is therefore not included in our source inventory.

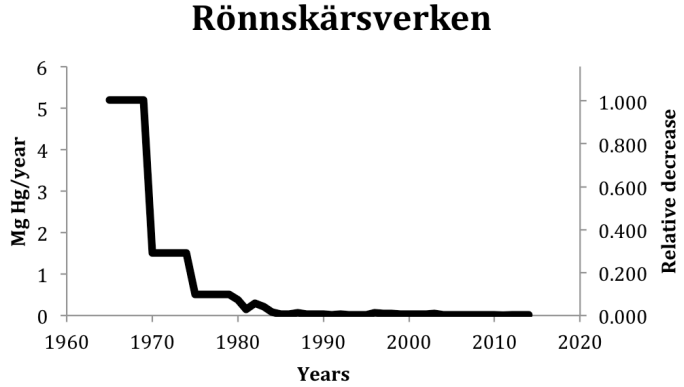

Reported changes in Hg discharge to water at the smelting facility Rönnskärsverken in the Bothnian Bay.[7]

Table S1. Yearly loads of dissolved and particle bound total Hg from rivers.

Basin	HELCOM* Mg y^{-1}	Specific rivers Mg y^{-1}	Model (2005-2014) Mg y^{-1}	Hg_T:TOC ng mg^{-1}	TSS[E] mg l^{-1}
Basin 1-3	0.07	n/a	0.07	0.22	5
Basin 4-6	0.02	n/a	0.02	0.22	5
Basin 7-9	0.11	1.72/1.99[A]	0.48	0.36	24
Basin 10	0.24	0.05[B]	0.16	0.22	4
Basin 11	0.22	0.06[C]	0.25	0.22	4
Basin 12	0.01	n/a	0.26	0.36	24
Basin 13	0.19	0.14[D]	0.21	0.22	7
Total	0.83	1.86	1.45		

* [12] 2006 loads that include both river disharge and point sources.

[A] River Pasleka: 0.06 Mg y^{-1}, River Leba: 0.29 Mg y^{-1}, River Lupawa: 0.12 Mg y^{-1}, River Slupia: 0.19 Mg y^{-1}, River Nemunas: 0.8 Mg y^{-1} [(13)], Vistula: 0.15 Mg y^{-1} /0.38 Mg y^{-1} (1.58 Mg y^{-1} in flood year)[14, 15], Oder River: 0.11-0.14 Mg y^{-1};(1996-1997; [16]);

[B] Dalälven: 0.05 Mg y^{-1} [(13)];

[C] River Kemijoki: 0.06 Mg y^{-1} [(13)];

[D] River Narva: 0.14 Mg y^{-1} [(13)].

[E] Best estimates based on TSS measurement from databases at GEMstat[17] and the Swedish University of Agricultural Sciences[9] including data from Vistula, Oder, Neva, Luleå, Nissan, Thorneälven.

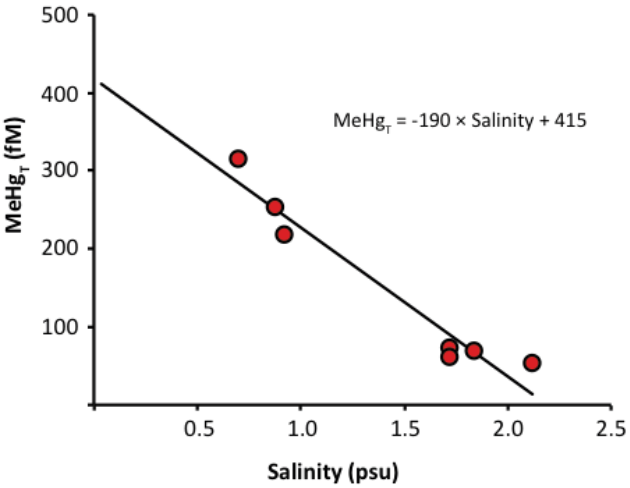

Figure S2. Extrapolation of $MeHg_T$ in Baltic Sea rivers. Data are from estuarine measurements in the Bothnian Bay 2015.

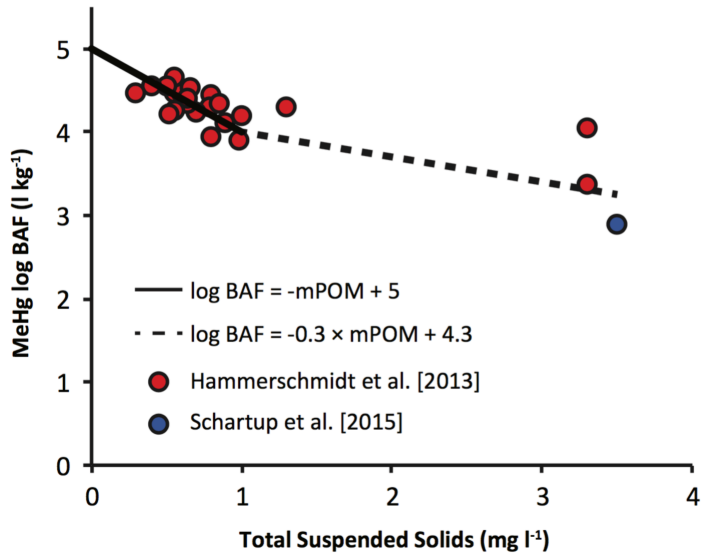

Figure S3. Linear equations for growth phytoplankton biodilution based on data from estuaries and continental margin of the Atlantic Ocean.[18, 19] Total suspended solids (TSS) observed by Hammerschmidt et al.[18] are assumed to be representative of autochthonous particular organic matter (mPOM) as they concluded that offshore TSS (0.2-200µm) was mostly of autochthonous origin.

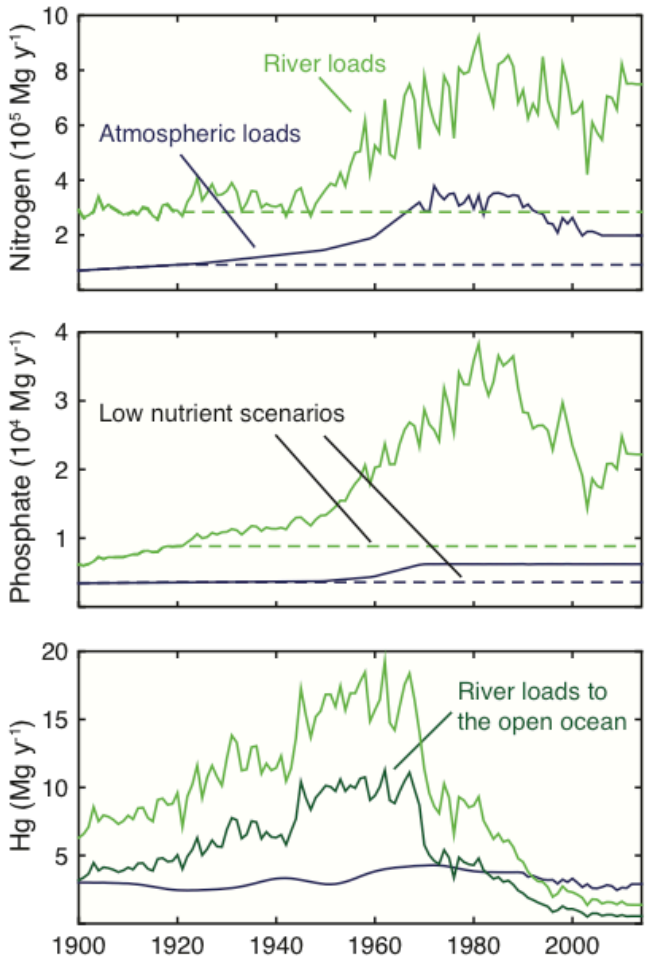

Figure S4. Baltic Sea historic atmospheric deposition and river discharge of nutrients and Hg used to drive the Baltsem model. The dark green line represents the fraction of the Hg in rivers that does not deposit right at the river mouth in the Baltic Sea (see Figure 1).

A

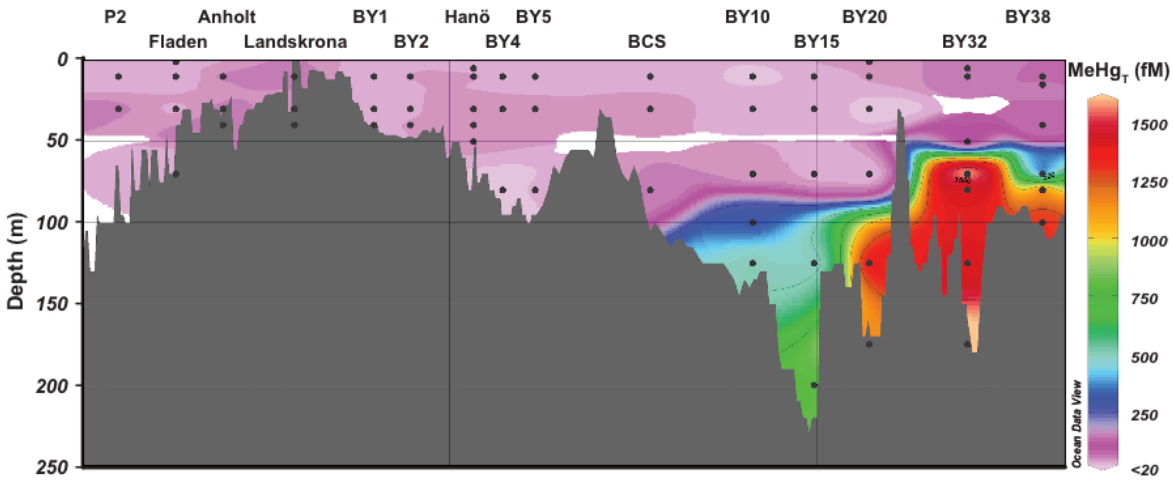

B

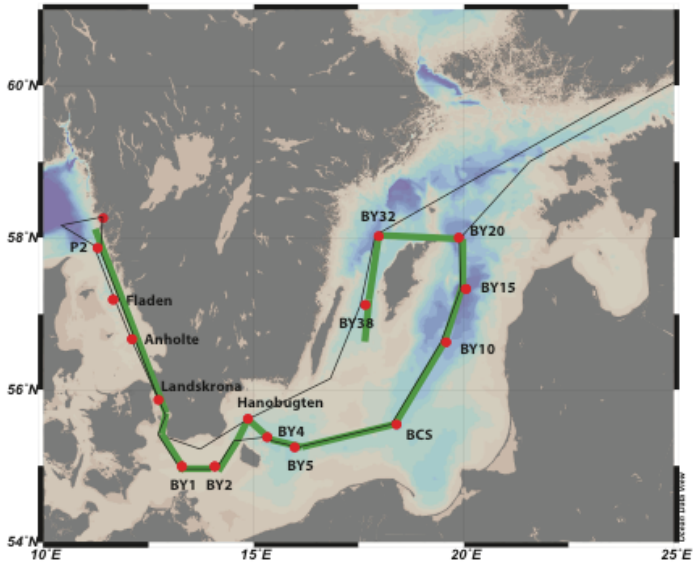

Figure S5. A) MeHg$_T$ concentrations and B) 2014 southern Baltic Sea cruise stations.

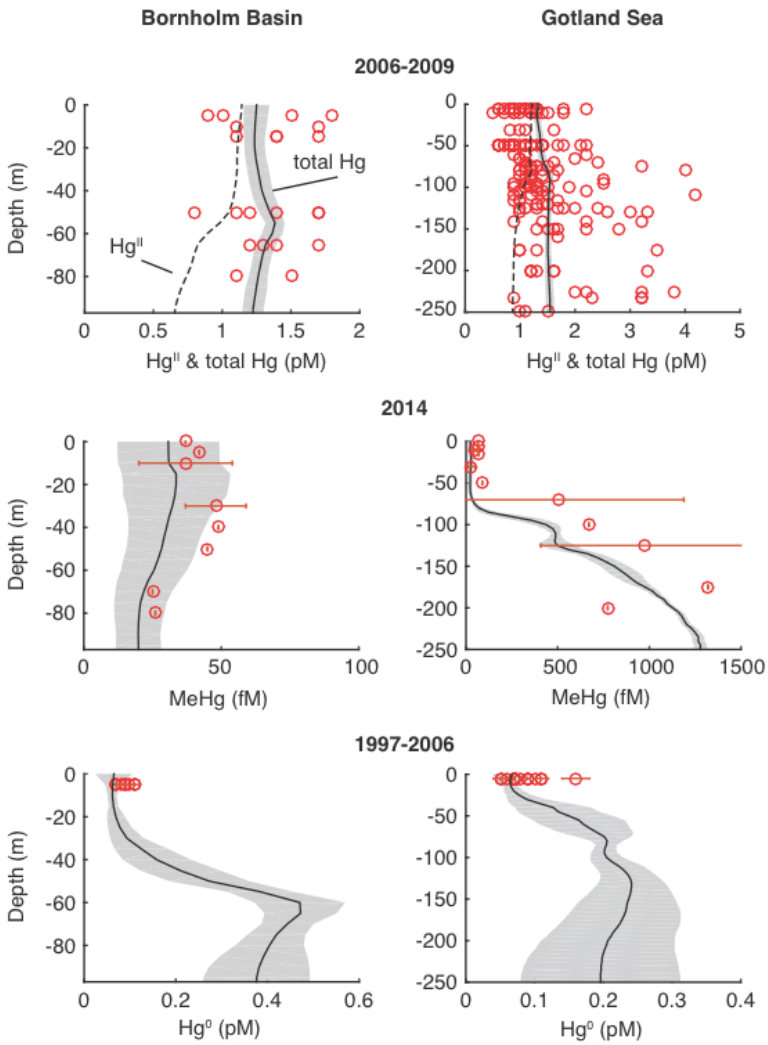

Figure S6. Comparison of observed and modeled Hg concentrations in the Bornholm Basin and the Gotland Sea. Hg_T data are from 2006-2009.[20] $MeHg_T$ data are from the 2014 cruise campaign described in TEXT S1. Hg^0 data are from Kuss and Schneider[21] and Wangberg et al.[22]. Modeled data for comparison are yearly averages from 2006-2009 for Hg_T and Hg^{II}, 2014 for $MeHg_T$ and 1997-2006 for Hg^0.

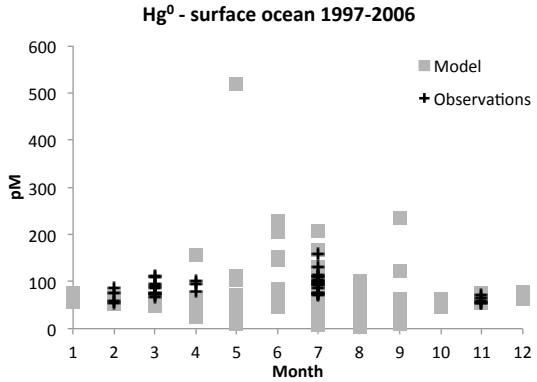

Figure S7. The seasonal variability of Hg^0 in observations and model simulation (modeled data from surface water in the Bornholm Basin). Modeled values are extracted from the model simulation two times a month at 0-1 m between 1997 and 2006. Observations are from 1997 and 2006.[21, 22] We find a significant correlation (R^2=0.53) between average monthly observations and model results over the 1997-2006 period.

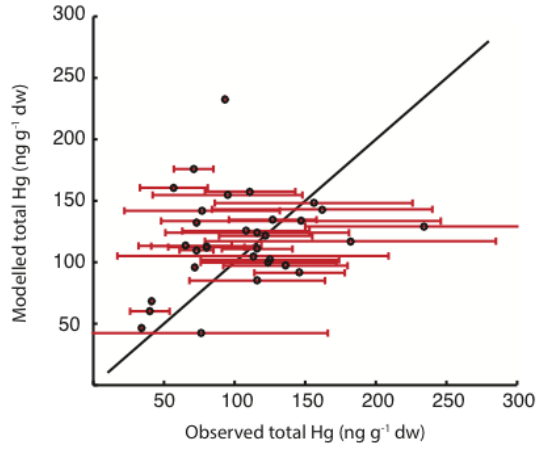

Figure S8. The figure compares observed and modeled total Hg data. Observed data is from Leipe et al.[6] and the Swedish Geological Investigations (1985-2011 sediment samples; Anna Apler, personal communication). The original samples were sorted by basin and divided into depth intervals (10 meters). When three or more samples were collected at a depth interval in a given basin a standard deviations was calculated. Only values with a standard deviation are used to calculate the percentage of modeled values within one standard deviation of observations. Observations are from six different basins and 1-13 depth intervals per basin.

Table S2. Average 2005-2014 difference between scenarios above the halocline (10-20 meters depth). The standard deviation is based on the variability between yearly averages.

	Bothnian Sea			Gotland Sea		
	Baseline	High nutrient	High:Base	Baseline	High nutrient	High:Base
Hg_{aq} (pM)	2.6±0.1	2.0±0.1	0.77	1.8±0.03	1.3±0.03	0.72
$MeHg_{aq}$ (fM)	16±2	23±4	1.44	15±1	24±3	1.53
$MeHg_{plankton}$ ($\times 10^6$ ng l^{-1})	6±1	18±6	3.00	12±4	42±12	3.50
$MeHg_{plankton}$ (ng g^{-1})	0.30±0.03	0.40±0.06	1.33	0.28±0.02	0.41±0.04	1.46

Table S3. Particulate organic matter **(**POM) and phytoplankton associated mercury (Hg) concentrations and fluxes.

$C_{p\text{-}HgII}$ (ng l^{-1})	THg concentration of POM	$C_{HgII} \times \phi_{HgII}$
$C_{p\text{-}MeHg}$ (ng l^{-1})	MeHg concentration of POM	$C_{MeHg} \times \phi_{MeHg}$
C_{Cyano} (ng l^{-1})	MeHg conc. in cyanobacteria	$C_{MeHg} \times \phi_{Cyano}$
C_{Diatom} (ng l^{-1})	MeHg conc. in diatoms	$C_{MeHg} \times \phi_{Diatom}$
C_{Flag} (ng l^{-1})	MeHg conc. in flagellates	$C_{MeHg} \times \phi_{Flag}$
F_{HgP} (ng d^{-1})	Hg^{II} detritus sinking flux	$C_{HgIIP} \times Det\_V \times A_{layer}$
F_{MeHgP} (ng d^{-1})	MeHg detritus sinking flux	$C_{MeHgP} \times Det\_V \times A_{layer}$
$F_{MeHg\text{-}Cyan}$ (ng d^{-1})	MeHg cyanobacteria sinking flux	$W_{Cyano} \times V_{Cyan} \times A_{layer}$
$F_{MeHg\text{-}Diatom}$ (ng d^{-1})	MeHg diatom sinking flux	$W_{Diatom} \times V_{Diatom} \times A_{layer}$
$F_{MeHg\text{-}Flag}$ (ng d^{-1})	MeHg flagellate sinking flux	$W_{Flag} \times V_{Flag} \times A_{layer}$
ϕ_{HgII} (unitless)	Hg^{II} fraction in the particulate phase	$1 - \left(\frac{1}{1 + K_{D-Hg} \times SPM}\right)$
ϕ_{MeHg} (unitless)	MeHg fraction in the particulate phase	$1 - \left(\frac{1}{1 + K_{D-MeHg} \times SPM}\right)$
ϕ_{Cyano} (unitless)	MeHg fraction in cyanobacteria	$1 - \left(\frac{1}{1 + BAF \times W_{cyano}}\right)$
ϕ_{Diatom} (unitless)	MeHg fraction in diatoms	$1 - \left(\frac{1}{1 + BAF \times W_{diatom}}\right)$
ϕ_{Flag} (unitless)	MeHg fraction in flagellates	$1 - \left(\frac{1}{1 + BAF \times W_{flag}}\right)$
$K_{D\text{-}Hg}$ (L kg^{-1})	Seawater partition coefficient for Hg^{II}	Log 5
$K_{D\text{-}MeHg}$ (L kg^{-1})	Seawater partition coefficient for MeHg	Log 4
BAF (L kg^{-1})	Seawater-plankton bioaccumulation factor	Equations given in Method section
W_{Cyano} (kg L^{-1})	Cyanobacteria WW concentration	$C_{c\text{-}cyano} \times M_{wet} \times 10^{-9}$
$W_{Diatoms}$ (kg L^{-1})	Diatom WW concentration	$C_{c\text{-}diatoms} \times M_{wet} \times 10^{-9}$
W_{Flag} (kg L^{-1})	Flagellate WW concentration	$C_{c\text{-}flag} \times M_{wet} \times 10^{-9}$
$C_{c\text{-}cyano}$ (mg m^{-3})	Standing stock of carbon in cyanobacteria	Model
$C_{c\text{-}diatoms}$ (mg m^{-3})	Standing stock of crbon in diatoms	Model
$C_{c\text{-}flag}$ (mg m^{-3})	Standing stock of carbon in flagellates	Model
M_{wet} (mg ww mg dw^{-1})	Dry weight (dw) to wet weights (ww) conversion	5 [23]
M_{dry} (mg dw mg C^{-1})	Organic carbon to dw conversion	2 [24, 25]
SPM (kg L^{-1})	Concentration of suspended particles	Model
Det_V (m d^{-1})	Detritus sinking velocity	Model
V_{Cyan} (m d^{-1})	Cyanobacteria sinking velocity	Model
V_{Diatom} (m d^{-1})	Diatom sinking	Model
V_{Flag} (m d^{-1})	Flagellate sinking velocity	Model
A_{layer} (m^2)	Area of layer	Model

Table S4. Water column chemistry

F_{ox} ($Mg\ d^{-1}$)	Oxidation flux	$M_{w\text{-}Hg0} \times (k_{dark\text{-}ox} + (k_{photo\text{-}ox} \times F_{open}))$
F_{red} ($Mg\ d^{-1}$)	Reduction flux	$M_{w\text{-}HgII} \times F_{red} \times (k_{bio\text{-}red} + (k_{photo\text{-}red} \times F_{open}))$
F_{met} ($Mg\ d^{-1}$)	Methylation flux	$M_{w\text{-}HgII} \times F_{red} \times (k_{met\text{-}nor} + k_{met\text{-}anox})$
F_{dem} ($Mg\ d^{-1}$)	Demethylation flux	$M_{w\text{-}MeHg} \times (k_{phot\text{-}dem} + k_{bio\text{-}dem})$
F_{met2} ($Mg\ d^{-1}$)	MeHg to Me_2Hg flux	$M_{w\text{-}MeHg} \times k_{met2}$
F_{2dec} ($Mg\ d^{-1}$)	Me_2Hg decomposition flux	$M_{w\text{-}Me2Hg} \times (k_{2dec} + k_{2dec\text{-}photo})$
$k_{phot\text{-}ox}$ (d^{-1})	Photo-oxidation rate constant	$0.55 \times RAD$ [26]
$k_{phot\text{-}red}$ (d^{-1})	Photo-reduction rate constant	$0.15 \times RAD$ [26]
$k_{dark\text{-}ox}$ (d^{-1})	Dark oxidation rate constant	0.02 [26]
$k_{bio\text{-}red}$ (d^{-1})	Biotic reduction rate constant	$0.01 \times DOM_{remin}$ (DOM_{remin}: 0-60) (max rate: 0.09)
$k_{met\text{-}nor}$ (d^{-1})	Methylation rate constant for normoxic water	WDCm / 100 (average rate 0.03% d^{-1})
$k_{met\text{-}anox}$ (d^{-1})	Methylation rate constant for hypoxic and anoxic water	$(PO_4 - PO_{4\text{-}base}) \times 5 \times 10^{-4}$ (max rate: 0.008) (if $O_2 < 2$ ml l^{-1})
$k_{phot\text{-}dem}$ (d^{-1})	Photo-demethylation rate constant	$PAR \times k_{phot\text{-}base} \times (-0.027 \times SAL + 1)$ [27]
$k_{phot\text{-}base}$ ($m^2\ E^{-1}$)	Photo-demethylation base rate constant	0.0025 [28]
$k_{bio\text{-}dem}$ (d^{-1})	Biotic demethylation rate constant	0.043 (2014 cruise observations)
k_{met2} (d^{-1})	MeHg to Me_2Hg rate constant	0.0003
k_{2dec} (d^{-1})	Me_2Hg dark decomposition rate constant	0.0082
$k_{2dec\text{-}photo}$ (d^{-1})	Me_2Hg photolytic decomposition rate constant	$PAR \times 1.08$ [29]
F_{red}	Fraction of reducible Hg^{II}	$0.45 - (9 \times 10^{-5} \times TDOM)$ based on Hg^0:THg relationships from Soerensen et al.[30]; Schartup et al.[19]
$F_{red\text{-}MeHg}$	Fraction of reducible MeHg	$0.75 - (9 \times 10^{-5} \times TDOM)$
F_{open}	Fraction of open ocean	Model
PAR ($E\ m^{-2}\ d^{-1}$)	Shortwave intensity as a function of time and depth	$RAD \times 0.432$
RAD ($W\ m^{-2}$)	Shortwave intensity as a function of depth	Model
$WDCm$ (d^{-1})	Particulate organic matter remineralization rate	Model
$PO_{4\text{-}base}$ ($\mu g\ L^{-1}$)	Concentration of PO_4 where Mn, Fe, and H_2S methylation begins	64.0
$TDOM$ ($\mu g\ L^{-1}$)	DOM from terrestrial sources	Model (basin averages 1000-3000 mg m^{-3})
DOM_{remin} (d^{-1})	DOM mineralisation rate	Model
SAL (psu)	Salinity of water	Model

Table S5. Sediment chemical transformation, water diffusion, and burial

$F_{sed\text{-}met}$ ($ng\ l^{-1}\ d^{-1}$)	Sediment methylation flux	$C_{psed\text{-}HgII} \times k_{sed\text{-}met}$
$F_{sed\text{-}dem}$ ($ng\ l^{-1}\ d^{-1}$)	Sediment demethylation flux	$C_{psed\text{-}MeHg} \times k_{sed\text{-}dem}$
$F_{sw\text{-}diff}$ ($ng\ m^{-2}\ d^{-1}$)	Diffusive flux based on Fick's law	$\frac{POR \times D_{sw} \times 10^{-4}}{TOR} \times \frac{\left(C_{psed-HgX} - C_{HgX}\right)}{D_{sed}/2} \times 10^{3} \times StoD$
F_{burial} ($ng\ m^{-2}\ d^{-1}$)	Burial flux of Hg^{II} and MeHg	$C_{sed} \times Burial \times Csedsolid \times 10^{6}$
$k_{sed\text{-}met}$ (d^{-1})	Sediment methylation rate constant	0.03 [31-33]
$k_{sed\text{-}dem}$ (d^{-1})	Sediment demethylation rate constant	4.0 (Derived based on the sediment MeHg:Hg^{II} ratio)
kd_{HgII}	Hg^{II} partitioning coefficient	2.97 + 0.15 * LOI (%) ($10^{3.1}$-$10^{4.0}$ [19, 23, 32])
kd_{MeHg}	MeHg partitioning coefficient	1.98 + 0.18 * LOI (%) ($10^{2.2}$-$10^{3.1}$ [19, 23, 32])
TOR	Tortuosity of sediments	$1 - \ln(POR^2)$ [34]
POR	Porosity of sediments	$1 - Csedsolid/dss$
$Csedsolid$ ($kg\ l^{-1}$)	Basin specific weight of solids per volume sediment	0.20-0.30 [35]
dss ($kg\ l^{-1}$)	Density of sediment solids	1.5
D_{sw} ($cm^2\ s^{-1}$)	Sediment-water diffusion coefficient at specific temperature	$O_2>0$: $D_{sw25} / (1+0.048\times(25-T_{sed}))$ $O_2<0$: $D_{swS25} / (1+0.048\times(25-T_{sed}))$ [34]
D_{sw25} ($cm^2\ s^{-1}$)	Sediment-water diffusion coefficient at 25 °C for ligand bound Hg complexes	2×10^{-6} [32]
D_{swS25} ($cm^2\ s^{-1}$)	Sediment-water diffusion coefficient at 25 °C for inorganic sulfide complexes	10×10^{-6} [32]
T_{sed} (°C)	Temperature of bottom water layer	Model
D_{sed} (m)	Depth of active layer	0.001
LOI (%)	Loss of ignition	$4.2854\times OC_{per} + 0.859$ [36]
Burial (d^{-1})	Shelf sediment burial rate	$k_{bur} \times OC/OC_{const}$
OC_{per} (%)	Organic carbon in sediment	Model
OC ($g\ m^{-2}$)	Organic carbon in sediment	Model
OC_{const} ($g\ m^{-2}$)	Constant OC baseline	80
k_{bur} (d^{-1})	Base burial rate	0.0006 (model)

Table S6. Gas exchange parameterization

F_v (ng m^{-2} h^{-1})	Hg^0 and Me_2Hg air-sea exchange flux	$K_W\left(\frac{C_{HgX}\times10^3 - C_a}{H'}\right) \times (1 - F_{ice})$
Ca_{Hg0} (ng m^{-3})	Concentration of Hg^0 in air	1.5 (current day)
Ca_{Me2Hg} (ng m^{-3})	Concentration of Me_2Hg in air	0.004 [37]
$H'_{Hg0}(T)$	Temperature dependent dimensionless Henry's law constant for Hg^0	$\ln H' = (\frac{-2403.3}{T} + 6.92)$ [38]
$H'_{Me2Hg}(T)$	Temperature dependent dimensionless Henry's law constant for Me_2Hg	$\ln H' = (\frac{-2512.43}{T} + 7.27)$ [39]
F_{ice}	Fraction of ocean covered by sea-ice	Model
K_w (m hr^{-1})	Water-side mass transfer coefficient	$A \times u_{10}^2 \left(\frac{Sc_{HgX}}{Sc_{CO2}}\right)^{-0.5}$ [40]
A (unitless)	Constant based on the Weibull distribution of wind speeds over oceans	0.25 [41]
u_{10} (m s^{-1})	Average wind speed at 10 m above sea surface	Model
Sc_{CO2}	Schmidt number for CO_2	$0.11T'^2 - 6.16T' + 644.7$ [42]
TK (K)	Water temperature	T′+273.15
T' (°C)	Water temperature	Model
$Sc_{HgX(0)}$	Schmidt number for Hg^0 and Me_2Hg	ν / D
ν (cm^2 s^{-1})	Kinematic viscosity	$N/\rho = 0.017e^{(-0.025T')}$ [42]
N (cP)	Viscosity of water	See Soerensen et al. [26]
ρ (mg cm^{-3})	Seawater density	1025
D_{kuss} (cm^2 s^{-1})	Hg^0 diffusivity based on Kuss et al. [43]	$0.0011 \times e^{-\frac{B}{(R\times TK)}}$
$D_{w\text{-}c}$ (cm^2 s^{-1})	Me_2Hg diffusivity based on Wilke-Chang [44]	$\frac{7.4\times10^{-8}(\phi_W M_W)^{0.5}\times TK}{NV_B^{0.6}}$
M_w (g mol^{-1})	Molecular weight of water	18.0
V_B (cm^3 mol^{-1})	Molal volume of Hg^0/Me_2Hg at its normal boiling temperature	12.74 / 72.11
ϕ_w	Solvent association factor	2.26 [45]
R (J/(mol K))	Gas constant	8.31446
B (J mol^{-1})	Constant	11.06×10^{-3} [43]

References

1. Lambertsson, L.; Bjorn, E. Validation of a Simplified Field-Adapted Procedure for Routine Determinations of Methyl Mercury at Trace Levels in Natural Water Samples Using Species-Specific Isotope Dilution Mass Spectrometry. *Anal. Bioanal. Chem.* **2004,** *380* (7-8), 871-875.
2. Munson, K. M.; Babi, D.; Lamborg, C. H. Determination of Monomethylmercury from Seawater with Ascorbic Acid-Assisted Direct Ethylation. *Limnol. Oceanogr. Methods* **2014,** *12,* 1-9.
3. Qvarnström, J.; Frech, W. Mercury Species Transformations During Sample Pre-Treatment of Biological Tissues Studied by Hplc-Icp-Ms. *J. Anal. Atom. Spectrom.* **2002,** *17* (11), 1486-1491.
4. Hintelmann, H.; Evans, R. Application of Stable Isotopes in Environmental Tracer Studies–Measurement of Monomethylmercury (CH3Hg+) by Isotope Dilution Icp-Ms and Detection of Species Transformation. *Fresen. J. Anal. Chem.* **1997,** *358* (3), 378-385.
5. Horowitz, H. M.; Jacob, D. J.; Amos, H. M.; Streets, D. G.; Sunderland, E. M. Historical Mercury Releases from Commercial Products: Global Environmental Implications. *Environ. Sci. Technol.* **2014,** *48* (17), 10242-10250; 10.1021/es501337j.
6. Leipe, T.; Moros, M.; Kotilainen, A.; Vallius, H.; Kabel, K.; Endler, M.; Kowalski, N. Mercury in Baltic Sea Sediments—Natural Background and Anthropogenic Impact. *Chem. Erde-Geochem.* **2013,** *73* (3), 249-259.
7. Borell, M.; Wik-Persson, M.; Åberg, L. *Miljörapport 2007, Rönnskärsverken Och Rönnskärs Hamn, RMS 8021,* 2008 (www.boliden.com/sv/).
8. Amos, H. M.; Jacob, D. J.; Kochman, D.; Horowitz, H. M.; Zhang, Y.; Dutkiewicz, S.; Horvat, M.; Corbitt, E. S.; Sunderland, E. M. Global Biogeochemical Implications of Mercury Discharges from Tivers and Sediment Burial. *Environ. Sci. Technol.* **2014,** *48* (16), 9514-9522; 10.1021/es502134t.
9. SLU, Institutionen För Vatten Och Miljö: Flodmynningar (1965-2013) (http://info1.ma.slu.se/ma/www_ma.acgi$ProjectP?ID=Intro&P=FLODMYNN), accessed: October 2014.
10. Naturvårdseverket *Wastewater Treatment in Sweden* Naturvårdsverket (Swedish Environmental Protection Agency)(www.naturvardsverket.se), 2014.
11. Szymczycha, B.; Miotk, M.; Pempkowiak, J. Submarine Groundwater Discharge as a Source of Mercury in the Bay of Puck, the Southern Baltic Sea. *Water Air Soil Poll.* **2013,** *224* (6), 1-14.
12. HELCOM *The Fifth Baltic Sea Pollution Load Compilation (Plc-5). Balt. Sea Environ. Proc. No. 128* (http://Helcom.Fi/Lists/Publications/Bsep128.Pdf), 2011.
13. HELCOM *Ecosystem Health of the Baltic Sea 2003-2007: Helcom Initial Holistic Assessment. Balt. Sea Environ. Proc. No 122* (www.Helcom.Fi/Lists/Publications/Bsep122.Pdf), 2010, p 63.
14. Saniewska, D.; Beidowska, M.; Beldowski, J.; Jedruch, A.; Saniewski, M.; Falkowska, L. Mercury Loads into the Sea Associated with Extreme Flood. *Environ. Pollut.* **2014,** *191*, 93-100; 10.1016/j.envpol.2014.04.003.
15. Beldowska, M.; Saniewska, D.; Falkowska, L. Factors Influencing Variability of Mercury Input to the Southern Baltic Sea. *Mar. Pollut. Bull.* **2014,** *86* (1-2), 283-290; 10.1016/j.marpolbul.2014.07.004.

16. Polak-Juszczak, L. Temporal Trends in the Bioaccumulation of Trace Metals in Herring, Sprat, and Cod from the Southern Baltic Sea in the 1994–2003 Period. *Chemosphere* **2009,** *76* (10), 1334-1339.
17. *Global Environment Monitoring System* (http://Www.Gemstat.Org/Queryrgn.Aspx*)*
18. Hammerschmidt, C. R.; Finiguerra, M. B.; Weller, R. L.; Fitzgerald, W. F. Methylmercury Accumulation in Plankton on the Continental Margin of the Northwest Atlantic Ocean. *Environ. Sci. Technol.* **2013**, *47* (8), 3671-3677; DOI 10.1021/es3048619.
19. Schartup, A. T.; Balcom, P. H.; Soerensen, A. L.; Gosnell, K. J.; Calder, R. S. D.; Mason, R. P.; Sunderland, E. M. Freshwater Discharges Drive High Levels of Methylmercury in Arctic Marine Biota. *PNAS* **2015,** *112* (38), 11789-11794; 10.1073/pnas.1505541112.
20. Pohl, C.; Hennings, U. *Trace Metal Concentrations and Trends in Baltic Surface and Deep Waters. Helcom Baltic Sea Environment Fact Sheet 2009* (online: http://Helcom.Fi/Baltic-Sea-Trends/Environment-Fact-Sheets/Hazardous-Substances/Trace-Metal-Concentrations-and-Trends-in-Baltic-Surface-and-Deep-Waters/*), Accessed March 2016*
21. Kuss, J.; Schneider, B. Variability of the Gaseous Elemental Mercury Sea-Air Flux of the Baltic Sea. *Environ. Sci. Technol.* **2007,** *41* (23), 8018-8023.
22. Wangberg, I.; Schmolke, S.; Schager, P.; Munthe, J.; Ebinghaus, R.; Iverfeldt, A. Estimates of Air-Sea Exchange of Mercury in the Baltic Sea. *Atmos. Environ.* **2001,** *35* (32), 5477-5484.
23. Sunderland, E. M.; Dalziel, J.; Heyes, A.; Branfireun, B. A.; Krabbenhoft, D. P.; Gobas, F. A. P. C. Response of a Macrotidal Estuary to Changes in Anthropogenic Mercury Loading between 1850 and 2000. *Environ. Sci. Technol.* **2010,** *44* (5), 1698-1704; 10.1021/Es9032524.
24. Redfield, A. C.; Ketchum, B. H.; Richards, F. A. The Influence of Organisms on the Composition of Seawater. In *The Sea, Vol. 2.*; Hill, M. N., Ed. Interscience: New York, 1963; pp 26-77.
25. Hedges, J. I.; Baldock, J. A.; Gelinas, Y.; Lee, C.; Peterson, M. L.; Wakeham, S. G. The Biochemical and Elemental Compositions of Marine Plankton: A NMR Perspective. *Mar. Chem.* **2002,** *78* (1), 47-63.
26. Soerensen, A. L.; Sunderland, E. M.; Holmes, C. D.; Jacob, D. J.; Yantosca, R. M.; Skov, H.; Christensen, J. H.; Strode, S. A.; Mason, R. P. An Improved Global Model for Air-Sea Exchange of Mercury: High Concentrations over the North Atlantic. *Environ. Sci. Technol.* **2010,** *44* (22), 8574-8580; 10.1021/Es102032g.
27. Kim, M.-K.; Won, A.-Y.; Zoh, K.-D. The Production of Dissolved Gaseous Mercury from Methylmercury Photodegradation at Different Salinity. *Desalination and Water Treatment* **2014**, *57* (2), 610-619.
28. Black, F. J.; Poulin, B. A.; Flegal, A. R. Factors Controlling the Abiotic Photo-Degradation of Monomethylmercury in Surface Waters. *Geochim. Cosmochim. Acta* **2012,** *84*, 492-507.
29. Soerensen, A. L.; Jacob, D. J.; Schartup, A.; Fisher, J. A.; Lehnherr, I.; St Louis, V. L.; Heimburger, L. E.; Sonke, J.; Krabbenhoft, D. P.; Sunderland, E. M. A Mass Budget for Mercury and Methylmercury in the Arctic Ocean. *Glob. Biogeochem. Cy.* **2016,** *30*; DOI 10.1002/2015GB005280.
30. Soerensen, A. L.; Mason, R. P.; Balcom, P. H.; Sunderland, E. M. Drivers of Surface Ocean Mercury Concentrations and Air-Sea Exchange in the West Atlantic Ocean. *Environ. Sci. Technol.* **2013,** *47*, 7757-7765; DOI 10.1021/ea401354q.

31. Heyes, A.; Mason, R. P.; Kim, E. H.; Sunderland, E. Mercury Methylation in Estuaries: Insights from Using Measuring Rates Using Stable Mercury Isotopes. *Mar. Chem.* **2006,** *102* (1-2), 134-147; DOI 10.1016/J.Marchem.2005.09.018.
32. Hollweg, T. A.; Gilmour, C. C.; Mason, R. P. Mercury and Methylmercury Cycling in Sediments of the Mid-Atlantic Continental Shelf and Slope. *Limnol. Oceanogr.* **2010,** *55* (6), 2703-2722.
33. Hammerschmidt, C. R.; Fitzgerald, W. F. Sediment-Water Exchange of Methylmercury Determined from Shipboard Benthic Flux Chambers. *Mar. Chem.* **2008,** *109* (1-2), 86-97.
34. Gill, G. A.; Bloom, N. S.; Cappellino, S.; Driscoll, C. T.; Dobbs, C.; McShea, L.; Mason, R.; Rudd, J. W. M. Sediment-Water Fluxes of Mercury in Lavaca Bay, Texas. *Environ. Sci. Technol.* **1999,** *33* (5), 663-669.
35. Jonsson, P. Sediment Burial of Pcbs in the Offshore Baltic Sea. *AMBIO: A Journal of the Human Environment* **2000,** *29* (4), 260-267.
36. Leipe, T.; Tauber, F.; Vallius, H.; Virtasalo, J.; Uścinowicz, S.; Kowalski, N.; Hille, S.; Lindgren, S.; Myllyvirta, T. Particulate Organic Carbon (Poc) in Surface Sediments of the Baltic Sea. *Geo-Marine Letters* **2011,** *31* (3), 175-188.
37. Baya, P. A.; Gosselin, M.; Lehnherr, I.; St Louis, V. L.; Hintelmann, H. Determination of Monomethylmercury and Dimethylmercury in the Arctic Marine Boundary Layer. *Environ. Sci. Technol.* **2015,** *49* (1), 223-232; DOI 10.1021/es502601z.
38. Andersson, M. E.; Gardfeldt, K.; Wangberg, I.; Stromberg, D. Determination of Henry's Law Constant for Elemental Mercury. *Chemosphere* **2008,** *73* (4), 587-592; DOI 10.1016/j.chemosphere.2008.05.067.
39. Lindqvist, O.; Rodhe, H. Atmospheric Mercury - a Review. *Tellus B.* **1985,** *37* (3), 136-159.
40. Wanninkhof, R. Relationship between Wind-Speed and Gas-Exchange over the Ocean. *J. Geosphys. Res. Oceans* **1992,** *97* (C5), 7373-7382.
41. Nightingale, P.; Malin, G.; Law, C.; AJ, W.; Liss, P.; Liddicoat, M.; Boutin, J.; Upstill-Goddard, R. In Situ Evaluation of Air-Sea Gas Exchange Parameterizations Using Novel Conservative and Volatile Tracers. *Glob. Biogeochem. Cy.* **2000,** *14* (1), 373-387.
42. Poissant, L.; Amyot, M.; Pilote, M.; Lean, D. Mercury Water-Air Exchange over the Upper St. Lawrence River and Lake Ontario. *Environ, Sci. Technol.* **2000,** *34* (15), 3069-3078.
43. Kuss, J. Water–Air Gas Exchange of Elemental Mercury: An Experimentally Determined Mercury Diffusion Coefficient for Hg0 Water-Air Flux Calculations. *Limnol. Oceanogr.* **2014,** *59 (5)*, 1461-1467.
44. Wilke, C. R.; Chang, P. Correlation of Diffusion Coefficients in Dilute Solutions. *Aiche J.* **1955,** *1* (2), 264-270.
45. Hayduk, W.; Laudie, H. Prediction of Diffusion-Coefficients for Nonelectrolytes in Dilute Aqueous Solutions. *Aiche J.* **1974,** *20* (3), 611-615.